



Published in final edited form as:

Arthritis Rheum. 2012 October ; 64(10): 3210–3219. doi:10.1002/art.34600.

Relationship between inflammation, bone destruction, and osteoproliferation in spondyloarthritis in HLA-B27/Hu β 2m transgenic rats

Leonie M. van Duivenvoorde, PhD^{1,2}, Martha L. Dorris, B.S.³, Nimman Satumtira, M.S.³, Melissa N. van Tok, B.S.^{1,2}, Kurt Redlich, MD, PhD⁴, Paul P. Tak, MD, PhD¹, Joel D. Taurog, MD³, and Dominique L. Baeten, MD, PhD^{1,2}

¹Department of Clinical Immunology and Rheumatology, Academic Medical Center/University of Amsterdam, Amsterdam, The Netherlands ²Department of Experimental Immunology, Academic Medical Center/University of Amsterdam, Amsterdam, The Netherlands ³Department of Internal Medicine, Rheumatic Diseases Division, UT Southwestern Medical Center, Dallas, TX, USA

⁴Department of Internal Medicine III, Division of Rheumatology, Medical University of Vienna, Vienna, Austria

Abstract

Objective—Inhibition of inflammation and destruction but not osteoproliferation in spondyloarthritis (SpA) patients treated with anti-TNF raises the question of how these three processes are interrelated. This study aimed to analyze this relationship in a SpA rat model.

Methods—Histological spine and joint samples of HLA-B27/Hu β 2m transgenic rats were analyzed for signs of spondylitis and destructive arthritis and semi-quantitatively scored as mild, moderate or severe inflammation.

Results—In spondylitis, mild inflamed sections displayed lymphocyte infiltration in connective tissue adjacent to the junction of the annulus fibrosus and vertebral bone but not at the enthesis. Moderate inflamed tissue samples contained osteoclasts eroding bone outside the cartilage endplate. In severe inflammation, the cartilage endplate and underlying bone marrow were also affected. End-stage disease was characterized by complete destruction of the intervertebral disc and vertebrae, with ongoing infiltration. Osteoproliferation was not observed in samples with no or mild inflammation, but was present at the edge of the vertebrae in moderate inflammation and persisted during severe inflammation and end-stage destruction. Osteoproliferation occurred at the border of inflammation, at a distance from bone destruction. A strong correlation between the extent of inflammation, destruction and osteoproliferation was observed. Arthritis displayed a similar pattern of synovial inflammation associated with bone destruction, and simultaneous but topographically distinct osteoproliferation starting from the periosteum.

Conclusion—Spondyloarthritis in HLA-B27/Hu β 2m tg rats is characterized by destructive inflammatory pannus tissue rather than by enthesitis or osteitis. Destruction and osteoproliferation occur simultaneously but at distinct sites in joints with moderate to severe inflammation.

Introduction

Spondyloarthritis (SpA) is the second most frequent form of chronic inflammatory arthritis. It comprises several closely related disorders, including ankylosing spondylitis, psoriatic arthritis, inflammatory bowel disease related spondyloarthritis, reactive arthritis, and undifferentiated spondyloarthritis (1). All these sub-forms of SpA are characterized by inflammation of the axial and/or peripheral skeleton, often in association with extra-articular inflammation of skin, gut, or eye. Moreover, SpA patients develop structural joint damage which, in contrast to rheumatoid arthritis (RA), is often characterized by the formation of bony spurs (axial syndesmophytes and peripheral osteophytes). Accumulating evidence indicates that this unique, distinctive structural phenotype of SpA is not related to the absence of cartilage and bone destruction (2), but rather to the marked presence of endochondral new bone formation (3). This osteoproliferation can ultimately lead to ankylosis. Inflammation, bone/cartilage destruction, and osteoproliferation are thus three main features of SpA pathogenesis. Over the last decade, human and experimental studies have yielded increasing insights in the cellular and molecular processes driving each of these features (4). However, the exact relationship among these three pathological processes remains unknown. Clinical trials with TNF blockers and animal studies have indicated that inflammation and osteoproliferation in SpA are at least partially disconnected, since effective suppression of inflammation by TNF blockade does not halt progression of new bone formation (5–8).

Two major hypotheses have been proposed to explain this disconnect. The first hypothesis proposes that new cartilage and bone formation is a form of (excessive) repair initiated by inflammation and joint destruction (9). The inflammation would initially trigger bone destruction and, simultaneously, suppress new bone formation. TNF plays a central role in this process as it promotes osteoclast differentiation and activation while suppressing osteoblast function by blocking *wingless* (Wnt) signaling (10). Upon resolution of the original inflammation, erosive damage triggers reactive osteoproliferation which, if unchecked, can lead to exaggerated new bone formation and ankylosis. Here, the relapsing/remitting type of inflammation, common in SpA would allow reparative new bone formation, whereas the chronic active state of inflammation, common in RA would not (9). If correct, this hypothesis predicts that late anti-inflammatory treatment would not affect or might even enhance osteoproliferation.

The second hypothesis proposes that an unknown trigger, presumably enthesal stress, induces simultaneously an acute inflammatory reaction and activation of stromal progenitor cells (11). The inflammation can develop into a chronic inflammatory process in which cytokines like TNF and interleukin (IL)-1 β play a pivotal role. The activation of stromal progenitor cells would lead to chondroid metaplasia, endochondral bone formation and, ultimately, new bone formation. In this scenario, inflammation and osteoproliferation are induced by the same trigger but proceed independently. Accordingly, prevention of structural remodeling would not necessarily be achieved by anti-inflammatory treatment, but would require specific targeting of the stromal remodeling pathways.

Testing these hypotheses remains difficult in human SpA because this requires i) diagnosis at the earliest stage of disease, ii) long-term prospective follow-up of new bone formation, and iii) histological analysis of the affected tissues, especially the spine. Analysis of SpA animal models partially circumvents these obstacles. In the present study, we used the HLA-B27 transgenic rat model to investigate the connection between inflammation, bone destruction, and osteoproliferation. HLA-B27/human beta-2 microglobulin (Hu- β 2m) transgenic rats develop a spontaneous multi-organ disease that resembles human SpA. In the original HLA-B27/Hu- β 2m tg disease-prone lines, all rats spontaneously developed diffuse

colitis, whereas only 20–40% developed arthritis, and spondylitis was rare (12;13). The low frequency of spondylitis precluded a thorough histological analysis of the structural joint remodeling. More recently, a second model was developed with fewer transgene copies of HLA-B27 and increased transgene copy numbers of Hu- β 2m (14). This model, in which 70% and 30–50% of the male rats spontaneously develop clinically apparent arthritis and spondylitis, respectively, without colitis induction, more closely resembles human SpA. The initial histological evaluation of full-blown disease in these rats showed inflammation, osteoclastic bone destruction and new bone formation in both axial and peripheral joints (14). Therefore, we used this transgenic model to perform a detailed histological analysis of the relationship between inflammation, tissue destruction and osteoproliferation in HLA-B27 associated disease.

Materials and methods

Rats

The transgenic 21-3 (HLA-B27/Hu β 2m) and 283-2 (Hu β 2m) rat lines (inbred Lewis background) were bred and maintained as previously described (12;14). Twenty-six diseased (21 \times 83-2)F1 rats, ages between 6–12 months, were used. For spondylitis tail samples of 10 rats were analyzed. For arthritis hind limbs from 19 and front paws from 4 animals were assessed, reaching a total of 24 arthritic paws. All animal experiments were performed at University of Texas Southwestern Medical Center and were approved by the Institutional Animal Care and Use Committee.

Sample processing and histological stainings

Paws and tail tissues were harvested, fixed, and sectioned as previously described (12). Briefly, joints were fixed overnight in 4% neutral buffered formalin, and decalcified in 14% EDTA. Samples were embedded in paraffin and cut to 5 μ M sections. Sections were deparaffinized and stained for 10' with Mayer's hematoxylin solution (Sigma-Aldrich, Zwijndrecht, The Netherlands). After rinsing with tap water and 96% ethanol, the sections were stained for 2' with accustain[®] eosin solution (Sigma-Aldrich), dehydrated, and mounted in entellan (Merck, Darmstadt, Germany). Alternatively, deparaffinized sections were stained with 0.04% Toluidine Blue (Sigma-Aldrich) in 0.2 M acetate buffer, pH 5.0 for 5–7', rinsed in distilled H₂O, dried 9' by air, dehydrated and mounted with entellan.

Histological analysis

Stained sections were scored by 3 independent observers (LMvD, MNvT and DLB). Based on similar histological studies of human synovial tissue (15;16), sections were semi-quantitatively graded based on the degree of lymphocyte infiltration: normal, mild, moderate, and severe. To assess the relationship between inflammation and structural damage, the same sections were analyzed for bone destruction and osteoproliferation.

Inflammation was graded 0–3, with 0 = healthy; 1 = mild inflammation with mono- and polynuclear cells infiltrating the connective tissue. 2 = moderate inflammation, the infiltrate progresses between the vertebrae and intervertebral disc. 3 = severe inflammation, also the vertebrae are infiltrated. Tissue destruction was also graded 0–3, with 0 = absence of multinucleated cells and erosions; 1 = multi-nucleated, osteoclast-like cells and erosions were observed at the edge of the vertebrae; 2 = osteoclast-like cells and erosions were present between the vertebrae and the intervertebral disc and 3 = osteoclast-like cells and erosions were present in the vertebral body. Osteoproliferation was also graded 0–3, with 0 = no remodeling; 1 = foci of hypertrophic chondrocytes at 1 location per intervertebral disc; 2 = foci of hypertrophic chondrocytes at 2 distinct locations per intervertebral disc, and 3 = foci at 3 or more locations per intervertebral disc. This quantitative analysis was performed

on 27 intervertebral discs by two independent observers (LMvD, MNvT). The scores were concordant in 81% of the cases. In 19% of the cases, the scores were discordant and the average of the two scores was used.

Statistical analysis

The correlation between the different processes was evaluated using linear regression analyses with a 95% confidence interval, Pearson rank correlations (r^2) and P values. P values below 0.05 were considered statistical significant.

Results

Absence of structural changes in non-inflamed axial joints of HLA-B27/Hu- β 2m transgenic rats

First non-inflamed axial joints were assessed to describe normal histology in the transgenic rats and to investigate whether bone destruction and/or osteoproliferation may be present in the absence of inflammation. In order to avoid bias due to age, we did not use young, healthy rats for this analysis but compared non-inflamed intervertebral discs from HLA-B27/Hu- β 2m transgenic rats with clinical tail spondylitis. We identified 10 intervertebral spaces without and 17 with inflammation. They were composed of intervertebral discs located between two vertebrae (Supplementary Figure 1A). The disc consisted of a cartilage-like nucleus pulposus which was contained laterally by the annulus fibrosus (Supplementary Figure 1B). The vertebrae were mainly composed of bony filaments and bone marrow located at both sides of the cartilaginous endplate (Supplementary Figure 1C and D). These structures were surrounded by connective tissue containing tendons and muscles (Supplementary Figure 1E). Systematic analysis of non-inflamed axial joints showed no evidence of cartilage damage, bone destruction or osteoproliferation, supporting the concept that inflammation is a prerequisite for these processes.

Inflammatory infiltration of the axial skeleton

We next assessed axial samples from clinically inflamed tail joints (n=17) and evaluated the degree, location, and type of inflammatory infiltration. In samples with a mild inflammation (n=5), the first infiltrating cells were consistently found in the connective tissue bordering the junction of the vertebral body with the annulus fibrosus. The vertebrae, the intervertebral discs and the site of insertion of the annulus fibrosus to the vertebra remained free of inflammation (Figure 1A and B). In moderate inflamed samples (n=6), the inflammation expanded from this edge into the surrounding connective tissue and into the bone between the cartilage endplate and the intervertebral disc (Figure 1C–D). At this stage, some samples also contained infiltrating cells in the bone marrow at the inner side of the cartilage endplate (Figure 1D), suggesting the presence of osteitis. In severe inflamed samples (n=6), the infiltrate affected not only the connective tissue but also the bone at both sides of the cartilage endplate and the disc tissues (Figure 1E). At all stages of inflammation, the infiltrate contained numerous neutrophils (Figure 1F). We did not observe any sign of enthesitis in any of the samples (Figure 1G). Together, these findings suggest that axial inflammation in HLA-B27/Hu- β 2m transgenic rats does not start as enthesitis or osteitis but progresses from the connective tissue at the edge of the vertebra and the annulus fibrosus.

Bone and cartilage destruction in spontaneous rat spondylitis

Next, we studied the relationship between spinal inflammation and tissue destruction. In samples with no or mild inflammation, no signs of cartilage or bone destruction were observed (data not shown). In contrast, all samples (6/6) with moderate inflammatory infiltration showed clear signs of bone destruction as osteoclast-like multinucleated giant

cells, eroding the bone, appeared at the edge of the inflammation (Figure 2A–B). At this stage, destruction was limited to the bone outside the cartilage endplate, which itself stayed intact. In all severe inflamed samples (6/6), bone erosions by multinucleated giant cells became more pronounced and were observed at both sides of the cartilage endplate (Figure 2C–D). Although the cartilage endplate and disc remained intact in half of the samples with severe inflammation, defects in the cartilage endplate could be observed in 3/6 samples. Finally, some samples (n=3) displayed destruction of the anatomical structure (Figure 2E–F). At this stage, distinction could not be made between vertebrae, intervertebral disc and connective tissue, since the discrete structures were obliterated. Interestingly, infiltrating immune cells and osteoclast-like cells were still abundant in these samples. In conclusion, these data indicate that tissue destruction occurs only in the presence of moderate to severe inflammation, starts at the bone outside the cartilage endplate, and gradually progresses.

Osteoproliferation in spontaneous rat spondylitis

We next analyzed the relationship between inflammation and osteoproliferation in spondylitis in HLA-B27/Hu β 2m transgenic rats. Samples with no or mild inflammation did not display histological signs of osteoproliferation (data not shown). In all samples (6/6) with moderate infiltration, foci of hypertrophic chondrocytes were seen in the connective tissue adjacent to the annulus fibrosus, at the outer border of ongoing inflammation and at a distance from bone degradation (Figure 3A–B). The foci were even more pronounced in samples with severe inflammation (6/6) (Figure 3C) or complete destruction (4/4) (Figure 3E). Toluidine blue staining confirmed that these foci consisted of hypertrophic chondrocytes producing a cartilage-like matrix (Figure 3D–F). This osteoproliferation, observed in all samples with moderate or severe inflammatory changes, always occurred in the connective tissue outside the intervertebral disc, but not at the place where the tendon is attached to the bone (entheses). In pronounced cases, this led to the formation of fully developed syndesmophytes, as depicted in Figure 3G, which nearly completely bridged the intervertebral space. These findings indicate that osteoproliferation i) does not occur in the absence of inflammation, ii) is ongoing during severe inflammation and destruction, and iii) is located at the border of the inflammation but affects a different anatomical site than the destruction.

Correlation between inflammation, tissue destruction and osteoproliferation

After careful description and anatomical localization of the different processes, we used a semi-quantitative histological score to assess the correlation between inflammation, destruction and osteoproliferation in spondylitis in HLA-B27/Hu β 2m tg rats. There was a strong, significant correlation between the degree of inflammation and tissue destruction ($r^2=0.9271$ and $P<0.0001$) (Figure 4A), between the degree of inflammation and osteoproliferation ($r^2=0.8317$ and $P<0.0001$) (Figure 4B), and the degree of tissue destruction and osteoproliferation ($r^2=0.9065$ and $P<0.0001$). This quantitative analysis confirmed the histological description indicating that both destruction and osteoproliferation occurred simultaneously in axial joints with moderate and severe inflammation but not in samples with no or mild inflammation (Figure 4D).

Peripheral arthritis in HLA-B27/Hu- β 2m transgenic rats

We next assessed whether a similar pattern of inflammation, bone destruction and osteoproliferation was observed in arthritis in these rats. Clinically uninvolved peripheral joints (n=4) did not show any signs of inflammation, joint destruction or remodeling (Figures 5A–B). In mild inflamed samples (n=6), the inflammation was consistently observed in the synovial membrane (Figure 5C). In more severe cases (n=5), this synovial inflammation extended into the articular cartilage and the subchondral bone, with progressive destruction of these structures (Figure 5D). Also the infiltrate in arthritis

contained numerous neutrophils. Besides destructive synovitis, the more severely affected joints (n=5) also displayed pronounced osteitis affecting bone marrow (Figure 5E). In a minority of cases (n=4) osteitis occurred in the absence of synovitis (data not shown). Severe cases of osteitis showed the presence of osteoclast-like multinucleated giant cells adjacent to the inner bone surfaces, suggesting that bone could be eroded by both synovial pannus and osteitis (Figure 5F). In contrast to synovitis and osteitis, none of the samples (n=24) displayed signs of enthesitis (data not shown). Regarding osteoproliferation, samples with moderate to severe synovitis and/or osteitis displayed large zones of hypertrophic chondrocytes emerging from the periosteum outside the joint (Figure 5G). Newly formed cartilage covered zones of progressive calcification and active bone remodeling as evidenced by the presence of osteoclast-like cells, suggesting a progressive ossification process (Figure 5H). These data indicate that arthritis is characterized by a destructive synovitis and osteitis, whereas primary enthesitis was not observed in the analyzed sections. Similar to axial disease, destruction and osteoproliferation occur together but at distinct anatomical sites in joints with moderate to severe inflammation.

Discussion

In this study the relationship between inflammation, bone destruction, and osteoproliferation was analyzed in the HLA-B27/Hu- β 2m (21-x83-2)F1 transgenic rat, which is a well validated animal model for SpA (14;17). Assessment of a high number of axial (n=27) and peripheral (n=24) joints at different disease stages allowed us to describe the exact anatomical localization of the pathology and to correlate the presence and extent of structural alterations with the degree of inflammation. The overall picture emerging from this analysis is schematically represented for axial disease in Figure 6. First, structural alterations are not found in the absence of inflammatory infiltration. Second, the infiltration starts in the connective tissue at the junction between the vertebral bone and the annulus fibrosus (Figure 6A). This early inflammation is not observed in either the bone marrow or the enthesis (including the insertion of the annulus fibrosus into the bone) and comprises numerous neutrophils. Moreover, there were no histological signs of bone destruction and/or osteoproliferation. Third, in samples with more pronounced inflammation, the infiltration extends to the vertebral bone outside the cartilage endplate (Figure 6B). This pannus-like tissue invades the bone and contains multiple osteoclast-like multinucleated giant cells which line the bone erosions. These samples also display signs of inflammation in the bone marrow despite an intact cartilage endplate, as well as new foci of hypertrophic chondrocytes outside the joint. Fourth, in severe inflammation, infiltration and bone destruction were not limited to the bone outside the cartilage endplate but also affected and destroyed the cartilage endplate itself and the bone marrow (Figure 6C). Also at this stage inflammatory pannus was characterized by multiple neutrophils and osteoclast-like cells. As the extent of inflammation and destruction increases, the foci of osteoproliferation outside the joint become larger and tend to progress over the joint space to form bridging osteophytes, even though we did not observe complete ankylosis in any of the samples analyzed. Finally, severe inflammation was associated with complete obliteration of all joint structures, including bone, cartilage endplate, annulus fibrosus and nucleus pulposus (Figure 6D). Outside this destructive inflammatory process we still observed ongoing osteoproliferation.

It needs to be emphasized that the description of these processes is based on a cross-sectional histological analysis and therefore it remains speculative to translate the variance in degree of inflammation and associated damage in a sequence of events. The low incidence (arthritis and spondylitis in 70% and 30–50%, respectively, of the males but none of the females) and variable onset of arthritis and spondylitis in this model does not allow a thorough sequential analysis over time. Albeit it is reasonable to assume that stages of mild

disease precedes moderate and severe disease, we can not exclude that some mildly affected joints will not progress or that more severe disease can partially resolve. We are currently optimizing this experimental model to increase the incidence and synchronize the onset of disease in order to be able to assess this sequence of events more formally (18). Independently of these limitations, our histological observations lead to 3 important conclusions. First, the inflammatory process primarily affects the stromal tissue and not the insertion of tendon and ligaments or the bone marrow. In line with previous data in human SpA synovitis, numerous neutrophils are observed in this inflammatory infiltrate (15;19–21). In spondylitis, this stromal site is the connective tissue at the border of the bone and the annulus fibrosus, whereas in arthritis it is the synovial tissue. Importantly, we consistently observed marked inflammation of these tissues without signs of infiltration of the insertion sites in the same sections. For example, we did not observe any infiltration of the insertion of the annulus fibrosus at the vertebrae despite strong inflammation of the surrounding connective tissue. Careful analysis of 27 axial and 24 peripheral joints did not reveal a single enthesial site with inflammation. Osteitis was seen in both axial and peripheral disease, but mostly at more severe stages of inflammation when the infiltration was expanding. This finding seems at odds with the hypothesis which proposes that enthesitis is the primary and unifying feature of SpA (22). This hypothesis was originally based on a MRI study of established SpA and RA patients with knee synovitis demonstrating that 10 of 10 patients with SpA had enthesitis whereas it was observed in only 4 of 10 RA patients (23). This concept might have important implications for understanding the role of mechanical stress in SpA (24), which is well illustrated by the ankylosing enthesitis model in male DBA/1 mice (25). The discrepancy between this concept and our current observations obviously emphasizes that experimental models should be used and interpreted carefully as they often recapitulate part but not all of the human disease. The present histological analysis does not argue against enthesitis as an important feature of human SpA but only indicates that this feature is not recapitulated in the HLA-B27/Hu- β 2m transgenic rat model. Independently of the caveats of experimental models, the current histological findings reminds us that the few studies that have attempted to reproduce the original human observations have yielded conflicting results (2), and detailed histological analysis of human sacroiliitis revealed synovitis rather than enthesitis (26;27). Osteitis and subchondral inflammation, which have also been described as principle features of early human SpA (26;28;29); are clearly observed in the HLA-B27/Hu- β 2m transgenic rats with moderate to severe inflammation. However, we must stress that we did not include the analysis of sacroiliac joints in the present study as one of our previous studies (14) showed very similar histological features in sacroiliac joints and tails, and as the processing and analysis of rat sacroiliac joints is technically challenging. Nevertheless, the data of the present study in HLA-B27/Hu- β 2m transgenic rats are thus in line with these histological data on human sacroiliitis and warrant more detailed studies of the presence of enthesitis versus synovitis and osteitis by histology and imaging in prospective studies of early SpA.

A second important conclusion is that severe stages of both axial and peripheral inflammation are characterized by an inflammatory pannus containing osteoclasts, which leads to severely erosive and destructive disease. It is well recognized in human SpA that arthritis of synovial joints leads to bone destruction, as evidenced by the severely destructive peripheral changes in the psoriatic arthritis subtype and the erosions in sacroiliitis. Accordingly, osteoclasts and osteoclast activating factors have been shown to be active at these sites of inflammation (29;32;33). However, it remains unknown whether this destructive process in human SpA is only observed in synovial joints, as in hTNF tg mice (10), or also extends to the vertebrae as seen in our model. In human peripheral SpA, it has also been shown that this erosive process is inflammation-driven, since TNF blockade is able to stop bone destruction in psoriatic arthritis, just as it does in RA (34–36). Whereas the anatomical co-localization and the strong correlation between the extent of inflammation

and destruction in the HLA-B27/Hu- β 2m transgenic rat strongly suggest that both processes are linked, formal demonstration of a causal relationship would require interventional studies with, for example, TNF blockade. As indicated for the sequential analysis over time, however, such studies cannot be performed in the current model due to the low incidence and variable time of disease onset. The third and most important conclusion is that the extent of osteoproliferation strongly correlates with the degree of inflammation and destruction but occurs at a distinct anatomical site just outside the affected joints. Indeed, osteoproliferation, in both axial and peripheral disease, is never seen in the absence of inflammatory changes and occurs together with destruction. These data are in line with the distinct topography of erosion and new bone formation in Achilles tendon enthesitis in human SpA (37). The location and anatomy of the osteoproliferative lesions is similar to the so-called syndesmophytes in human SpA but, as we did not observe complete ankylosis of any of the analyzed axial or peripheral joints, it remains unsure whether these lesions completely mimic the human pathology. Nevertheless, the features of osteoproliferation in this experimental model can help to shed new light on the two major hypotheses on new bone formation in SpA discussed previously (9;11), as histology of axial and peripheral lesions of the transgenic rats clearly indicates a strong correlation between inflammation and osteoproliferation in this model as well as in the “old” HLA-B27/Hu β 2m transgenic rat model on the 33–3 background (12;38). However, these data do not indicate whether osteoproliferation is driven by inflammation (9) or whether osteoproliferation and inflammation are two independent processes initiated by a single pathogenic trigger (11). Despite the distinct anatomical localization of destruction and remodeling, they also do not formally indicate whether early erosive changes are required for the induction of osteoproliferation or not. This would require active intervention targeting inflammatory and/or destructive pathways early after onset of the disease process, as has been done previously in the ankylosing enthesitis model (8;39) and in adjuvant-induced arthritis model in rats (40). Keeping in mind the limitations of a cross-sectional histological analysis and the absence of interventional studies in this model, our data still indicate, that initiation and progression of osteoproliferation does not require complete resolution of the inflammatory process in the HLA-B27/Hu β 2m tg rat model.

In summary, the data in this study suggest that the spontaneously occurring spondyloarthritis in HLA-B27/Hu- β 2m tg rats is characterized by a destructive inflammatory pannus rather than by enthesitis or osteitis. Destruction and osteoproliferation occur simultaneously in joints with moderate to severe inflammation but not in non- or mild inflamed joints. This suggests a link between inflammation and joint damage but the exact causal relationship remains to be determined by interventional studies. The distinct anatomical localization of destruction and new bone formation and the presence of osteoproliferation despite ongoing severe inflammation do not support the concept of a reparative remodeling upon resolution of inflammation.

Supplementary Material

Refer to Web version on PubMed Central for supplementary material.

Acknowledgments

This project was funded by the Dutch Arthritis Association; an unrestricted grant from Abbott to the Spondyloarthritis Immunopathology Research Alliance (Spiral); and by NIH grant R01AR38319 (JDT). LMvd received personal funding from EMBO (ASTF 202.00-2010). DLB is supported by a Vidi grant from the Netherlands Scientific Organization (NWO).

References

1. Khan MA. Update on spondyloarthropathies. *Ann Intern Med.* 2002; 136(12):896–907. [PubMed: 12069564]
2. Vandooren B, Yeremenko N, Noordenbos T, Bras J, Tak PP, Baeten D. Mediators of structural remodeling in peripheral spondylarthritis. *Arthritis Rheum.* 2009; 60(12):3534–45. [PubMed: 19950262]
3. Lories RJ, Baeten DL. Differences in pathophysiology between rheumatoid arthritis and ankylosing spondylitis. *Clin Exp Rheumatol.* 2009; 27(4 Suppl 55):S10–S14. [PubMed: 19822039]
4. Dougados M, Baeten D. Spondyloarthritis. *Lancet.* 2011; 377(9783):2127–37. [PubMed: 21684383]
5. Schett G, Landewe R, van der Heijde D. Tumour necrosis factor blockers and structural remodelling in ankylosing spondylitis: what is reality and what is fiction? *Ann Rheum Dis.* 2007; 66(6):709–11. [PubMed: 17513569]
6. van der Heijde D, Landewe R, Einstein S, Ory P, Vosse D, Ni L, et al. Radiographic progression of ankylosing spondylitis after up to two years of treatment with etanercept. *Arthritis Rheum.* 2008; 58(5):1324–31. [PubMed: 18438853]
7. van der Heijde D, Landewe R, Baraliakos X, Houben H, van Tubergen A, Williamson P, et al. Radiographic findings following two years of infliximab therapy in patients with ankylosing spondylitis. *Arthritis Rheum.* 2008; 58(10):3063–70. [PubMed: 18821688]
8. Lories RJ, Derese I, de Bari C, Luyten FP. Evidence for uncoupling of inflammation and joint remodeling in a mouse model of spondylarthritis. *Arthritis Rheum.* 2007; 56(2):489–97. [PubMed: 17265484]
9. Sieper J, Appel H, Braun J, Rudwaleit M. Critical appraisal of assessment of structural damage in ankylosing spondylitis: implications for treatment outcomes. *Arthritis Rheum.* 2008; 58(3):649–56. [PubMed: 18311819]
10. Diarra D, Stolina M, Polzer K, Zwerina J, Ominsky MS, Dwyer D, et al. Dickkopf-1 is a master regulator of joint remodeling. *Nat Med.* 2007; 13(2):156–63. [PubMed: 17237793]
11. Lories RJ, Luyten FP, de Vlam K. Progress in spondylarthritis. Mechanisms of new bone formation in spondyloarthritis. *Arthritis Res Ther.* 2009; 11(2):221. [PubMed: 19439035]
12. Hammer RE, Maika SD, Richardson JA, Tang JP, Taurog JD. Spontaneous inflammatory disease in transgenic rats expressing HLA-B27 and human beta 2m: an animal model of HLA-B27-associated human disorders. *Cell.* 1990; 63(5):1099–112. [PubMed: 2257626]
13. Taurog JD, Maika SD, Satumtira N, Dorris ML, McLean IL, Yanagisawa H, et al. Inflammatory disease in HLA-B27 transgenic rats. *Immunol Rev.* 1999; 169:209–23. [PubMed: 10450519]
14. Tran TM, Dorris ML, Satumtira N, Richardson JA, Hammer RE, Shang J, et al. Additional human beta2-microglobulin curbs HLA-B27 misfolding and promotes arthritis and spondylitis without colitis in male HLA-B27-transgenic rats. *Arthritis Rheum.* 2006; 54(4):1317–27. [PubMed: 16575857]
15. Baeten D, Kruithof E, De Rycke L, Vandooren B, Wyns B, Boullart L, et al. Diagnostic classification of spondylarthropathy and rheumatoid arthritis by synovial histopathology: a prospective study in 154 consecutive patients. *Arthritis Rheum.* 2004; 50(9):2931–41. [PubMed: 15457462]
16. Baeten D, Demetter P, Cuvelier C, Van den Bosch F, Kruithof E, Van Damme N, et al. Comparative study of the synovial histology in rheumatoid arthritis, spondyloarthropathy, and osteoarthritis: influence of disease duration and activity. *Ann Rheum Dis.* 2000; 59(12):945–53. [PubMed: 11087697]
17. Taurog JD. Animal models of spondyloarthritis. *Adv Exp Med Biol.* 2009; 649:245–54. [PubMed: 19731634]
18. van Duivenvoorde LM, Slobodin GM, Satumtira N, Dorris ML, Tak PP, Baeten DL, et al. Innate Immune Stimulation Triggers Early-Onset Spondyloarthritis in HLA-B27/Human beta2 Microglobulin Transgenic Rats. *Arthritis and Rheumatism.* 2011; 63(10):S387.
19. Baeten D, Kruithof E, De Rycke L, Boots AM, Mielants H, Veys EM, et al. Infiltration of the synovial membrane with macrophage subsets and polymorphonuclear cells reflects global disease activity in spondyloarthropathy. *Arthritis Res Ther.* 2005; 7(2):R359–R369. [PubMed: 15743484]

20. Kruithof E, Baeten D, De Rycke L, Vandooren B, Foell D, Roth J, et al. Synovial histopathology of psoriatic arthritis, both oligo- and polyarticular, resembles spondyloarthritis more than it does rheumatoid arthritis. *Arthritis Res Ther.* 2005; 7(3):R569–R580. [PubMed: 15899044]
21. Kruithof E, Van den Bossche V, De Rycke L, Vandooren B, Joos R, Canete JD, et al. Distinct synovial immunopathologic characteristics of juvenile-onset spondylarthritis and other forms of juvenile idiopathic arthritis. *Arthritis Rheum.* 2006; 54(8):2594–604. [PubMed: 16868982]
22. McGonagle D, Gibbon W, Emery P. Classification of inflammatory arthritis by enthesitis. *Lancet.* 1998; 352(9134):1137–40. [PubMed: 9798608]
23. McGonagle D, Gibbon W, O'Connor P, Green M, Pease C, Emery P. Characteristic magnetic resonance imaging enthesal changes of knee synovitis in spondylarthritis. *Arthritis Rheum.* 1998; 41(4):694–700. [PubMed: 9550479]
24. McGonagle D, Lories RJ, Tan AL, Benjamin M. The concept of a “synovio-enthesal complex” and its implications for understanding joint inflammation and damage in psoriatic arthritis and beyond. *Arthritis Rheum.* 2007; 56(8):2482–91. [PubMed: 17665450]
25. Lories RJ, Matthys P, de Vlam K, Derese I, Luyten FP. Ankylosing enthesitis, dactylitis, and onychoprosperiostitis in male DBA/1 mice: a model of psoriatic arthritis. *Ann Rheum Dis.* 2004; 63(5):595–8. [PubMed: 15082495]
26. Francois RJ, Gardner DL, Degraeve EJ, Bywaters EG. Histopathologic evidence that sacroiliitis in ankylosing spondylitis is not merely enthesitis. *Arthritis Rheum.* 2000; 43(9):2011–24. [PubMed: 11014351]
27. Muche B, Bollow M, Francois RJ, Sieper J, Hamm B, Braun J. Anatomic structures involved in early- and late-stage sacroiliitis in spondylarthritis: a detailed analysis by contrast-enhanced magnetic resonance imaging. *Arthritis Rheum.* 2003; 48(5):1374–84. [PubMed: 12746910]
28. Gong Y, Zheng N, Chen SB, Xiao ZY, Wu MY, Liu Y, et al. Ten years' experience with needle biopsy in the early diagnosis of sacroiliitis. *Arthritis Rheum.* 2012; 64(5):1399–406. [PubMed: 22076932]
29. Appel H, Maier R, Loddenkemper C, Kayser R, Meier O, Hempfing A, et al. Immunohistochemical analysis of osteoblasts in zygapophyseal joints of patients with ankylosing spondylitis reveal repair mechanisms similar to osteoarthritis. *J Rheumatol.* 2010; 37(4):823–8. [PubMed: 20156950]
30. Redlich K, Hayer S, Maier A, Dunstan CR, Tohidast-Akrad M, Lang S, et al. Tumor necrosis factor alpha-mediated joint destruction is inhibited by targeting osteoclasts with osteoprotegerin. *Arthritis Rheum.* 2002; 46(3):785–92. [PubMed: 11920416]
31. Uderhardt S, Diarra D, Katzenbeisser J, David JP, Zwerina J, Richards W, et al. Blockade of Dickkopf (DKK)-1 induces fusion of sacroiliac joints. *Ann Rheum Dis.* 2010; 69(3):592–7. [PubMed: 19304568]
32. Ritchlin CT, Haas-Smith SA, Li P, Hicks DG, Schwarz EM. Mechanisms of TNF-alpha- and RANKL-mediated osteoclastogenesis and bone resorption in psoriatic arthritis. *J Clin Invest.* 2003; 111(6):821–31. [PubMed: 12639988]
33. Vandooren B, Cantaert T, Noordenbos T, Tak PP, Baeten D. The abundant synovial expression of the RANK/RANKL/Osteoprotegerin system in peripheral spondylarthritis is partially disconnected from inflammation. *Arthritis Rheum.* 2008; 58(3):718–29. [PubMed: 18311801]
34. Gladman DD, Mease PJ, Ritchlin CT, Choy EH, Sharp JT, Ory PA, et al. Adalimumab for long-term treatment of psoriatic arthritis: forty-eight week data from the adalimumab effectiveness in psoriatic arthritis trial. *Arthritis Rheum.* 2007; 56(2):476–88. [PubMed: 17265483]
35. Kavanaugh A, Antoni CE, Gladman D, Wassenberg S, Zhou B, Beutler A, et al. The Infliximab Multinational Psoriatic Arthritis Controlled Trial (IMPACT): results of radiographic analyses after 1 year. *Ann Rheum Dis.* 2006; 65(8):1038–43. [PubMed: 16439444]
36. van der Heijde D, Kavanaugh A, Gladman DD, Antoni C, Krueger GG, Guzzo C, et al. Infliximab inhibits progression of radiographic damage in patients with active psoriatic arthritis through one year of treatment: Results from the induction and maintenance psoriatic arthritis clinical trial 2. *Arthritis Rheum.* 2007; 56(8):2698–707. [PubMed: 17665424]
37. McGonagle D, Wakefield RJ, Tan AL, D'Agostino MA, Toumi H, Hayashi K, et al. Distinct topography of erosion and new bone formation in achilles tendon enthesitis: implications for

- understanding the link between inflammation and bone formation in spondylarthritis. *Arthritis Rheum.* 2008; 58(9):2694–9. [PubMed: 18759270]
38. Milia AF, Ibba-Manneschi L, Manetti M, Benelli G, Generini S, Messerini L, et al. Evidence for the prevention of enthesitis in HLA-B27/hbeta(2)m transgenic rats treated with a monoclonal antibody against TNF-alpha. *J Cell Mol Med.* 2011; 15(2):270–9. [PubMed: 20015205]
 39. Lories RJ, Derese I, Luyten FP. Inhibition of osteoclasts does not prevent joint ankylosis in a mouse model of spondyloarthritis. *Rheumatology (Oxford).* 2008; 47(5):605–8. [PubMed: 18334523]
 40. Schett G, Stolina M, Dwyer D, Zack D, Uderhardt S, Kronke G, et al. Tumor necrosis factor alpha and RANKL blockade cannot halt bony spur formation in experimental inflammatory arthritis. *Arthritis Rheum.* 2009; 60(9):2644–54. [PubMed: 19714640]
 41. Daoussis D, Lioussis SN, Solomou EE, Tsanakti A, Bounia K, Karampetsou M, et al. Evidence that Dkk-1 is dysfunctional in ankylosing spondylitis. *Arthritis Rheum.* 2010; 62(1):150–8. [PubMed: 20039407]

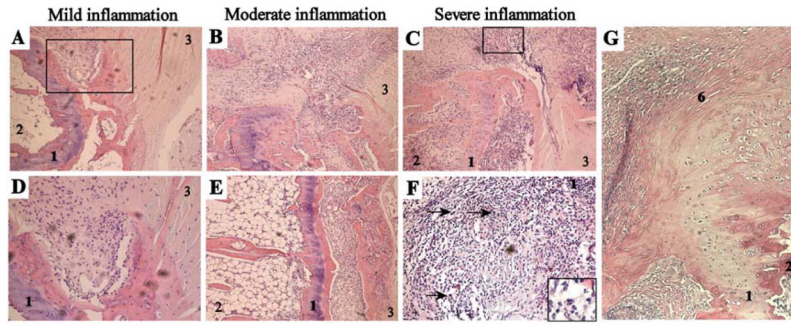


Figure 1. Histological analysis of inflammation in spondylitis
All photos are from H&E stained paraffin sections of axial joints. **A+D**, Mild inflammation, with cells infiltrating the connective tissue located at the junction of the bone and the annulus fibrosus. Panel A represents a 100x magnification and picture D is a larger magnification (500x) of the rectangle depicted in picture A. **B+E**, Moderate inflammation (100x magnification), showing progression of the inflammatory pannus in the bone outside of the cartilage endplate. **C+F**, Severe inflammation, affecting the connective tissue as well as the bone on both sides of the cartilage endplate. Panel C represents a 100x magnification and picture F is a larger magnification (500x) of the rectangle depicted in picture C. Arrows and the insert in picture F indicate neutrophils. **G**. Non-inflamed enthesis, next to moderate inflamed connective tissue (100x magnification) 1-cartilage endplate, 2-bone with bone marrow, 3-annulus fibrosus, 6-enthesis.

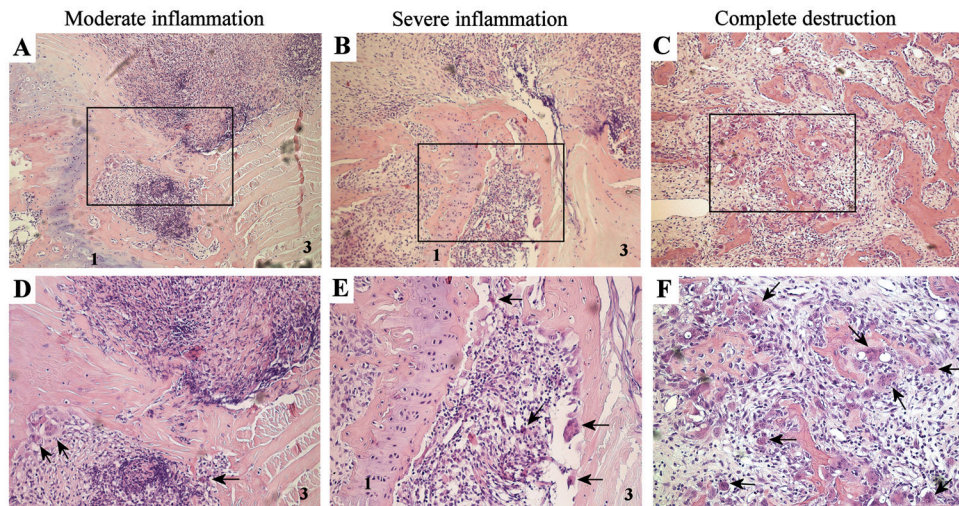


Figure 2. Histological analysis of tissue destruction in spondylitis

Overview of moderate inflammation (**A+D**), severe inflammation (**B+E**) and complete destruction (**C+F**). Panel A, B and C are 100x magnifications and panel D, E and F represent larger magnifications (500x) of the rectangles within, respectively, panel A, B and C. Arrows point towards multinucleated giant cells at the edge between the inflammatory pannus and the bone. All photographs are H&E stainings. 1-cartilage endplate, 3-annulus fibrosus.

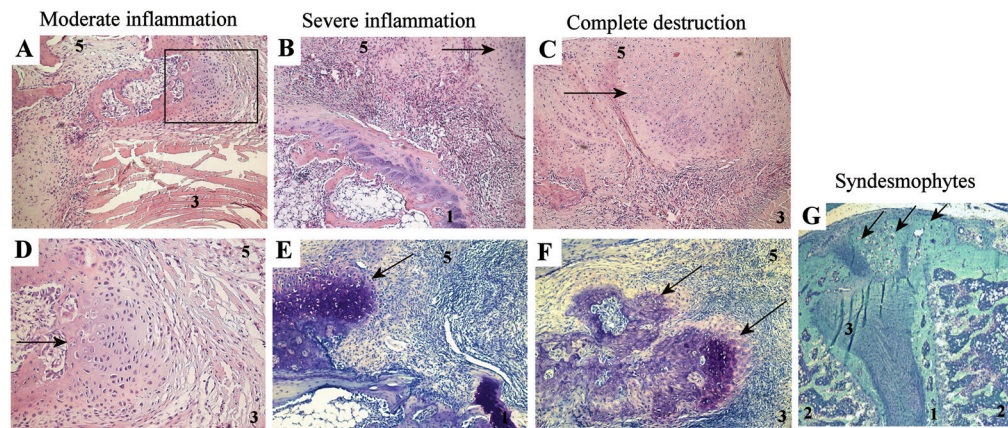


Figure 3. Histological analysis of osteoproliferation in spondylitis

Overview of moderate inflammation (A+D), severe inflammation (B+E), complete destruction (C+F) and syndesmophyte formation (G). Panel A, B, C and D are H&E stainings; panel E, F and G are toluidine blue stainings. All panels are at 100x magnification, except panel D at 500x, which is a magnification of the rectangle in panel A, and panel G at 25x magnification. Arrows point towards foci of hypertrophic chondrocytes and new formation or syndesmophytes (panel G), which are typically located outside the joint. 1-cartilage endplate, 2-bone with bone marrow, 3-annulus fibrosus, 5-connective tissue.

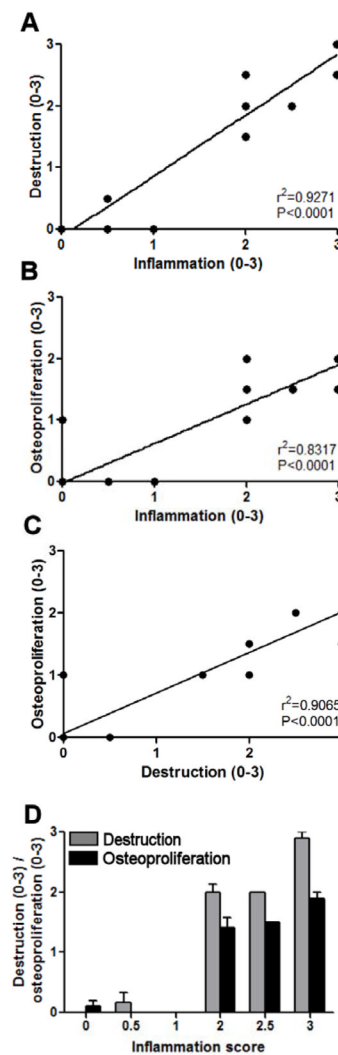


Figure 4. Quantification of inflammation, bone destruction and osteoproliferation

All three processes were scored using a 0–3 quantitative scoring system and every intervertebral disc was scored separately (in total 27 discs). **A**, Correlation between inflammation and tissue destruction is depicted ($r^2=0.9271$ and $P<0.0001$). **B**, Correlation between inflammation and osteoproliferation is depicted ($r^2=0.8317$ and $P<0.0001$). **C**, Correlation between destruction and osteoproliferation is depicted ($r^2=0.9065$ and $P<0.0001$). **D**, Tissue destruction and osteoproliferation are analyzed compared to the inflammation score. Values depicted are mean and SEM.

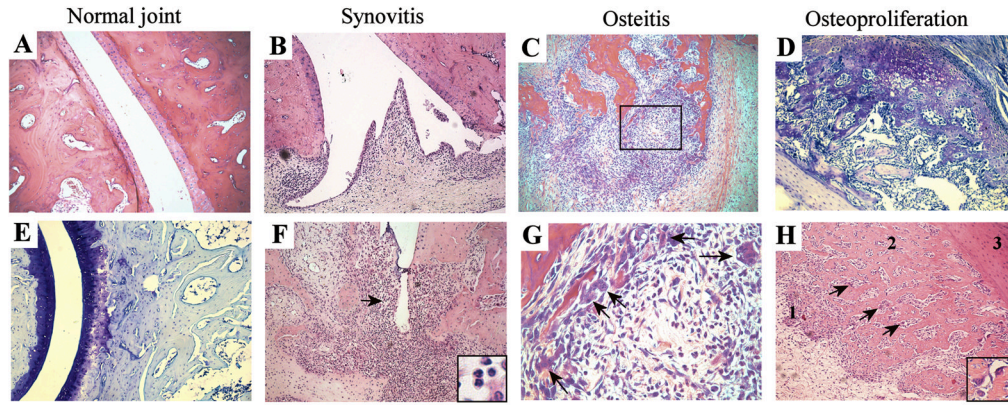


Figure 5. Histological analysis of peripheral joint disease

A+E. healthy joints. 100x magnifications, A is an H&E and E a toluidine blue staining. Depicted are bone structures, including cartilage. There are no signs of inflammatory infiltration, bone or cartilage destruction, or osteoproliferation. **B+F,** synovitis. Inflammation starts with progressive infiltration of the synovial membrane with leucocytes (panel B). As inflammatory infiltrate extends, pannus-like tissue starts to invade and destroy bone (panel F). The arrow and insertion in panel F display neutrophils. Both panels are 100x magnification H&E stainings. **C+G,** osteitis. In samples with extensive synovitis, inflammatory infiltration also affects bone marrow. C is a 100x magnified H&E staining and G is a more magnified (500x) photo of the rectangle depicted in C. Arrows point towards multinucleated giant cells. **D,** osteoproliferation. D represents a 100x magnification toluidine blue staining. Arrows point towards the foci of hypertrophic chondrocytes and bone remodeling starting from the periosteum at some distance of the joint. H represents an overview H&E staining (100x magnification): 1-the occurrence of hypertrophic chondrocytes; 2-formation of new bone, here both hypertrophic chondrocytes and osteoclasts were observed, and 3-bone. Arrows and insert display multinucleated giant, osteoclast-like cells.

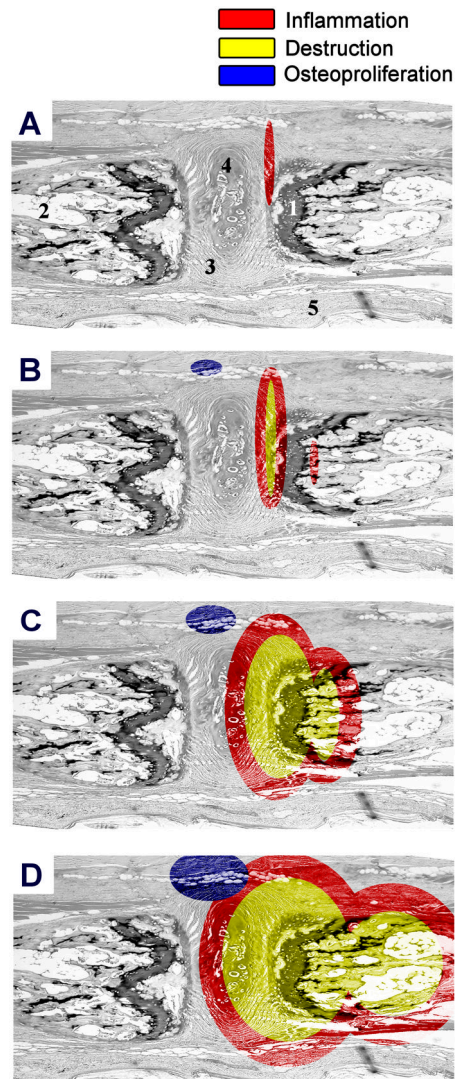


Figure 6. Schematic overview of axial disease

A, inflammation starts in the connective tissue neighboring the annulus fibrosus and the bone. No destruction or osteoproliferation is observed at this stage. **B**, when the inflammation progresses, the infiltrate gradually begins to affect the bone outside the cartilage endplate. At this stage of moderate inflammation, multinucleated giant cells appear and start to erode the bone. At the same time, the first foci of hypertrophic chondrocytes and new bone formation appear, but outside the joint. **C**, in severe inflammation, the erosive pannus-like tissue invades the cartilage endplate and the underlying bone marrow. This stage is characterized by the presence of numerous osteoclast-like multinucleated giant cells in the inflammatory zone as well as pronounced osteoproliferation outside this zone. **D**, even when the joint is completely destroyed and normal anatomical structures are obliterated, the processes of inflammation, destruction and osteoproliferation are still ongoing. Red: inflammation, yellow: bone destruction and blue: bone remodeling. The numbers indicate: 1-cartilage endplate, 2-bone with bone marrow, 3-annulus fibrosus, 4-nucleus pulposus, 5-connective tissue.